COMMUNICATION

Computational Mapping of Redox-Switchable Metal Complexes Based on Ferrocene Derivatives

Amy Lai,[a] Jamie Clifton,[b] Paula L. Diaconescu,*[a] Natalie Fey*[b]

Received 00th January 20xx,
Accepted 00th January 20xx

DOI: 10.1039/x0xx00000x

DFT calculations were used to capture the properties of redox-switchable metal complexes relevant to the ring-opening polymerisation of cyclic esters by varying the metals, donors, linkers, and substituents in both accessible ferrocene oxidation states. A map of this chemical space highlights that modifying the ligand architecture and the metal has a larger impact on structural changes than changing the oxidation state of the ferrocene backbone.

Computational mechanistic studies and databases of property descriptors calculated with standard approaches are increasingly used not just to analyse reaction mechanisms, but also to design catalyst screening, evaluate novel designs prior to synthesis, and guide optimisations.[1] Efforts to use regression models that predict reaction selectivity[2] and guide ligand design[1a, 3] have emerged as an important area of research in organic synthesis, especially related to organometallic catalysis. However, until recently,[4] studies that focussed on quantifying supporting ligand effects in early transition metal catalysis were lacking.

Cyclic ester/ether ring-opening polymerisation catalysts based on a redox-switchable ferrocene unit **1**-**12** (Chart 1), as reported by the Diaconescu group[5] and others,[6] present considerable challenges for a systematic computational screening. While the metallocene "switch" is shared by these tetradentate supporting ligands, the catalytically active metal, along with donors, linkers, and substituents of the supporting ligand may be varied (Figure 1), altering the activity and selectivity in ring-opening polymerisation reactions for a range of cyclic esters and ethers, including lactide, ε-caprolactone, and cyclohexene oxide.

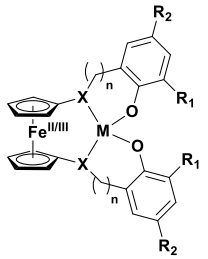

1 M = Ce(O*t*Bu)$_2$, X = N=PPh$_2$, n = 0, R$_1$ = *t*Bu,
2 M = Y(O*t*Bu), X = N=PPh$_2$, n = 0, R$_1$ = *t*Bu, R$_2$ = H
3 M = Zr(O*t*Bu)$_2$, X = NMe, n = 1, R$_1$ = R$_2$ = *t*Bu
4 M = Zr(O*t*Bu)$_2$, X = S, n = 1, R$_1$ = R$_2$ = *t*Bu
5 M = Ti(O*i*Pr)$_2$, X = S, n = 0, R$_1$ = R$_2$ = *t*Bu
6 M = Y(OAr), X = S, n = 1, R$_1$ = R$_2$ = *t*Bu
7 M = Ti(O*i*Pr)$_2$, X = N=CH, n = 0, R$_1$ = R$_2$ = *t*Bu
8 M = Al(O*t*Bu), X = S, n = 0, R$_1$ = R$_2$ = *t*Bu
9 M = In(OPh), X = N=PPh$_2$, n = 0, R$_1$ = *t*Bu, R$_2$ = H
10 M = Zr(O*t*Bu)$_2$, X = S, n = 0, R$_1$ = R$_2$ = *t*Bu
11 M = In(O*t*Bu), X = N=CH, n = 0, R$_1$ = R$_2$ = *t*Bu
12 M = Zr(O*i*Pr)$_2$, X = N=CH, n = 0, R$_1$ = R$_2$ = *t*Bu

Chart 1. Reported metal alkoxide complexes supported by a ferrocene chelating derivative.

In line with these observations, mechanistic studies of likely intermediates[5i, 7] and proposed catalytic cycles[5b, 5g, 5h] hint at a considerable diversity of coordination geometries and reaction pathways, further complicated when the metallocene oxidation state is changed. Due to this mechanistic complexity, computational evaluations of proposed reaction pathways can be useful for the interpretation of data, but are unlikely to achieve a timely prediction across the accessible variations.

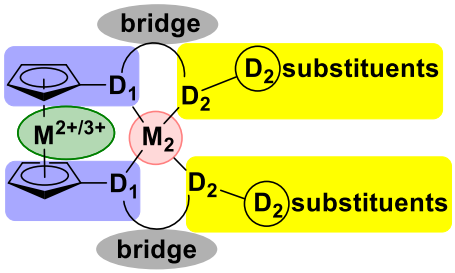

Figure 1. Variables for catalyst optimisation

[a] Department of Chemistry and Biochemistry, University of California, Los Angeles, California 90095, United States. Email: pld@chem.ucla.edu.
[b] School of Chemistry, University of Bristol, Cantock's Close, Bristol, BS8 1TS, UK. Email: Natalie.Fey@Bristol.ac.uk.

Electronic Supplementary Information (ESI) available: List of complexes and labels, computational details, database design, PCA results, table of descriptors and PC scores, sample input files. See DOI: 10.1039/x0xx00000x

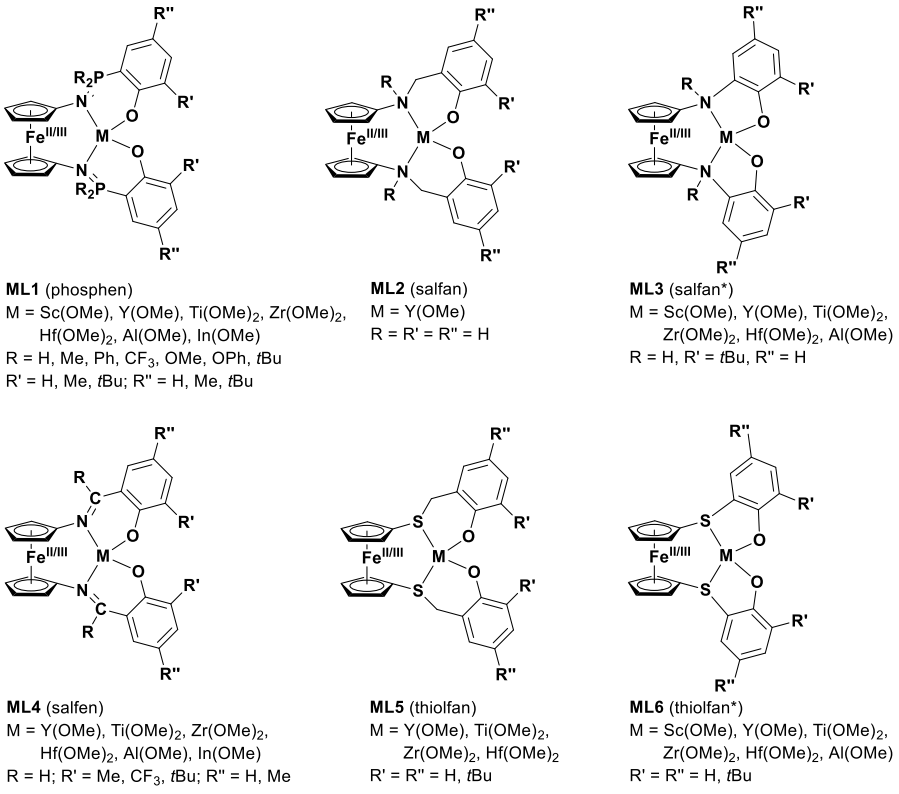

Chart 2. Overview of metal complexes considered and labelling scheme.

Following on from work on ligand knowledge bases[8] and descriptor-led characterisation of the alkyne/vinylidene tautomeric pair[9] reported previously, we became interested in exploring whether the *in silico* characterisation of metal complexes could be achieved from calculations on a representative scaffold, with a view to providing an accessible computational approach for mapping this chemical space.[1a, 8d]

To allow the consideration of subtle electronic modifications of catalyst properties at a reasonable computational cost, all calculations used a standard density functional and basis set combination (UB3PW91/6-31G(d), LACV3P* on metals, see ESI). In total, 64 different metal complexes were considered for each oxidation state, sampling seven metals (Sc(III), Y(III), Ti(IV), Zr(IV), Hf(IV), Al(III), In(III)) and six supporting ligand architectures (128 examples total). Chart 2 defines the compound labelling and variations explored, while Table S1 lists all metal complexes considered. From these optimisations, the descriptors shown in Table 1 were extracted. Database design and computational challenges are discussed in depth in the supporting information (page S5). We initially considered treating each oxidation state as a separate entry in the database, but found that the distribution of metal complexes in the Fe(II) and Fe(III) version tended to shadow rather closely (see Figure S1), making the data analysis difficult.

Table 1: Descriptors extracted for analysis. All calculations were performed on isolated molecules, see ESI for computational details. Fe2 refers to the ferrocene complex with Fe(II) in the backbone, while Fe3 refers to the ferrocenium complex, where this has been oxidised to Fe(III).

Descriptor	Details (unit)
M-D1(Fe2), M-D1(Fe3)	r(M-D1), both oxidation states (Å)
M-D2(Fe2), M-D2(Fe3)	r(M-D2), both oxidation states (Å)
M-OMe(Fe2), M-OMe(Fe3)	r(M-OMe), both oxidation states (Å)
D1-R(Fe2), D1-R(Fe3)	av. r(D1-R), both oxidation states (Å)
D2-R(Fe2), D2-R(Fe3)	r(D2-R), both oxidation states (Å)
∠R-D1-R(Fe2), ∠R-D1-R(Fe3)	av. ∠R-D1-R, both oxidation states (°)
Q(M)(Fe2), Q(M)(Fe3)	NBO charge on M, both oxidation states
Q(OMe)(Fe2), Q(OMe)(Fe3)	NBO charge on OMe group, both oxidation states
ΔFe-C	change in av. Fe-C distances due to oxidation state, av. r(Fe-C,Fe3) – av. r(Fe-C,Fe2) (Å)
ΔQ(Fe)	change in NBO charge on Fe centre, Q(Fe3) – Q(Fe2)
ΔE	E_{opt}(Fe3 complex) – E_{opt}(Fe2 complex) (kcal mol^{-1})

The resulting database of descriptors for redox-switchable catalysts was processed with principal component analysis

(PCA) to aid visualisation. Applications of this approach, often used in image processing, to databases of calculated descriptors have been discussed in detail elsewhere.[10] In brief, PCA is a statistical method designed to minimise the dimensionality of data sets while maximising the information content of fewer, orthogonal, i.e., uncorrelated variables (principal components, PCs) than those originally considered.

In the present case, the first two PCs capture around 56% of the variation in the dataset, while PC3 adds a further 14%. Figure 2 shows a plot of the first two PCs coloured by the supporting ligand (Chart 2), and another plot representing the same data coloured by the metal. Descriptor loadings can be found in the ESI (page S9), along with full diagnostics.

These PCA maps (Figure 2) highlight the main sources of variation in the database: a clear clustering can be observed based on the supporting ligand according to the donor atom D1, with ligands containing N occupying the lower half of the score plot (PC2<1) and those containing S nearer the top (PC2>1). Metal-donor distance descriptors load highly on both PC1 and PC2 (see Table S6 and Figure S2), indicating the importance of such structural changes to the observed variation. S donor supporting ligands were found to accommodate much longer M-D1 distances in the corresponding metal complexes, exceeding the sum of van der Waals radii for this interaction. For L3 (salfan*), the shorter bridge length compared to the other N-donor ligands (L1, L2, L4) also affects the coordination of this atom, leading to long M-D1 distances in these compounds. L3 metal complexes thus lie a little closer to the sulphur-containing L5 and L6 in the chemical space.

The plot based on the identity of the metal illustrates that a horizontal separation on this map arises, with Y(III), In(III), Zr(IV), and Hf(IV) complexes observed at smaller PC1 and larger PC2, while Al(III), Sc(III), and Ti(IV) complexes occur at larger PC1 and smaller PC2 values, in line with the changes in M-D1 distances for each case. We note that changing the metal also affects a range of other descriptors, most notably Q(M), M-OMe, and Q(OMe), which all load highly on PC1, helping to explain the clear response in terms of compound properties as highlighted by the PC score plot. Ligand structural variation was sampled most extensively for the yttrium complexes here, and these changes also affect coordination behaviour, as would be expected. Compound properties can be fine-tuned by changing from electron-donating to electron-withdrawing groups, most notable on the phosphorus in phosphen ligands, but variation of the R' substituent on the aryl ring, from *t*-butyl to CF_3 groups, will also achieve structural changes.

While changing the oxidation state of the ferrocene backbone affects the average Fe-C distances, with subsequent structural changes across the corresponding metal complex, a transmission of these effects to the reacting metal centre is relatively limited, showing much smaller changes to the M-OMe distances, Q(M), and Q(OMe) between the two oxidation states. We note, however, that the descriptors capturing a net change, i.e., ΔE, ΔQ(Fe), and ΔFe-C, show some variation across these compounds, suggesting that the response to oxidation state change in terms of structures and energies needs to be explored further.

PC3 captures an additional 14% of the variation in this dataset (see Figure S2 and Table S6 for descriptor loadings and Figure S11 for the PC1/PC3 score plot). M-D1, ΔQ(Fe), and both D2-R distances load highly on PC3, suggesting that changes in the ligand architecture/bridge length may be captured in this dimension; indeed, L3 appears separate from the other N-donor supporting ligands.

The most responsive variables for catalyst modification can be identified from this analysis and their effect quantified. Figure 3 shows the PC1/PC2 score compound map, coloured according to the charges on the methoxy groups that were used as a reporter potentially relevant to transmitted electronic changes in catalysis. The distribution across the map relates strongly to the identity of M.

The positions of metal complexes known to show catalytic activity on Figure 2 (marked in special red symbols) indicate that there is not a single supporting ligand or metal centre to be singled out, in agreement with reported experimental results that show that switchable catalysts range from group 4 to 13 metals and encompass different variations of the supporting ligand.

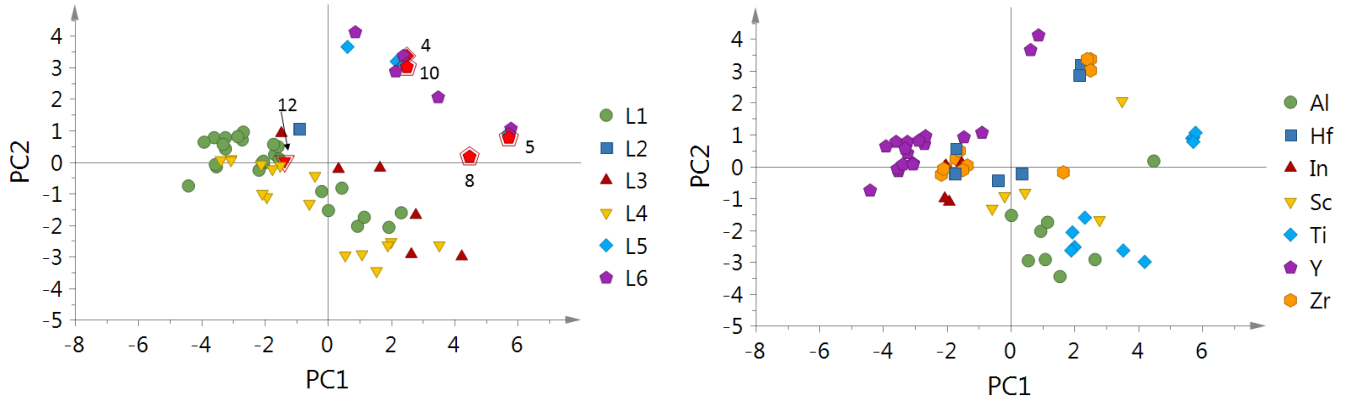

Figure 2: Left: Principal component score plot (PC1 and PC2) for metal complexes considered, capturing 56% of variation in the data. Plot generated by analysis of the full database of 19 variables (Table 1) for 64 redox pairs of metal complexes. Each symbol corresponds to one supporting ligand, colours and shapes relate to metal complexes (Chart 2). Symbols marked in bright red correspond to close analogues of compounds found active in ring-opening polymerisation catalysis, see Chart 1 above for numbering used. Right: The same plot as on the left but with colours and shapes corresponding to M. See ESI for both versions of this figure with full compound labels.

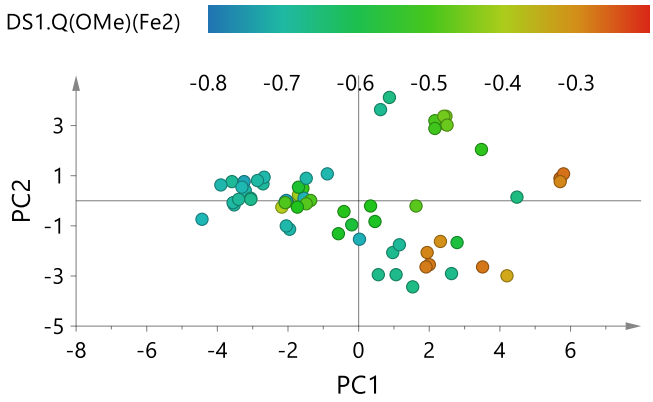

Figure 3: PC score plot (PC1 & PC2) coloured according to Q(OMe) (Fe2).

In conclusion, the present map and the underlying data demonstrate that a descriptor-led approach is feasible to support experimental design[11] and guide a sampling of the catalyst space. While changing the oxidation state of the ferrocene backbone does not have a major *structural* impact between the forms of a catalyst, the descriptors capturing a *net change*, i.e., ΔE, ΔQ(Fe), and ΔFe-C, are important and will be used in the future to refine the interpretation of experimental data. Work is currently under way to improve the method and to supplement the current descriptor database with extensive mechanistic studies, in order to construct suitable predictive models.

Acknowledgments

AL and PLD thank the National Science Foundation (Grant CHE-1809116) for supporting this work.

Conflicts of interest

There are no conflicts to declare.

Notes and references

1. a) D. J. Durand and N. Fey, *Chem. Rev.*, 2019, DOI: 10.1021/acs.chemrev.8b00588; b) J. Jover and N. Fey, *Chem. Asian J.*, 2014, **9**, 1714-1723.

2. a) K. C. Harper, E. N. Bess and M. S. Sigman, *Nat. Chem.*, 2012, **4**, 366–374; b) K. C. Harper and M. S. Sigman, *Proc. Nat. Acad. Sci.*, 2011, **108**, 2179–2183; c) P. S. Engl, C. B. Santiago, C. P. Gordon, W.-C. Liao, A. Fedorov, C. Copéret, M. S. Sigman and A. Togni, *J. Am. Chem. Soc.*, 2017, **139**, 13117-13125; d) M. Orlandi, J. A. S. Coelho, M. J. Hilton, F. D. Toste and M. S. Sigman, *J. Am. Chem. Soc.*, 2017, **139**, 6803-6806; e) Z. L. Niemeyer, S. Pindi, D. A. Khrakovsky, C. N. Kuzniewski, C. M. Hong, L. A. Joyce, M. S. Sigman and F. D. Toste, *J. Am. Chem. Soc.*, 2017, **139**, 12943-12946; f) J.-Y. Guo, Y. Minko, C. B. Santiago and M. S. Sigman, *ACS Catal.*, 2017, **7**, 4144-4151; g) M. Orlandi, M. J. Hilton, E. Yamamoto, F. D. Toste and M. S. Sigman, *J. Am. Chem. Soc.*, 2017, **139**, 12688-12695; h) C. B. Santiago, A. Milo and M. S. Sigman, *J. Am. Chem. Soc.*, 2016, **138**, 13424-13430; i) M. S. Sigman, K. C. Harper, E. N. Bess and A. Milo, *Acc. Chem. Res.*, 2016, **49**, 1292-1301.

3. a) K. Wu and A. G. Doyle, *Nat. Chem.*, 2017, **9**, 779-784; b) Z. L. Niemeyer, A. Milo, D. P. Hickey and M. S. Sigman, *Nat. Chem.*, 2016, **8**, 610-617.

4. B. S. Billow, T. J. McDaniel and A. L. Odom, *Nat. Chem.*, 2017, **9**, 837-842.

5. a) E. M. Broderick, N. Guo, C. S. Vogel, C. Xu, J. Sutter, J. T. Miller, K. Meyer, P. Mehrkhodavandi and P. L. Diaconescu, *J. Am. Chem. Soc.*, 2011, **133**, 9278-9281; b) E. M. Broderick, N. Guo, T. Wu, C. S. Vogel, C. Xu, J. Sutter, J. T. Miller, K. Meyer, T. Cantat and P. L. Diaconescu, *Chem. Commun.*, 2011, **47**, 9897-9899; c) X. Wang, A. Thevenon, J. L. Brosmer, I. Yu, S. I. Khan, P. Mehrkhodavandi and P. L. Diaconescu, *J. Am. Chem. Soc.*, 2014, **136**, 11264-11267; d) S. M. Quan and P. L. Diaconescu, *Chem. Commun.*, 2015, **51**, 9643-9646; e) X. Wang, J. L. Brosmer, A. Thevenon and P. L. Diaconescu, *Organometallics*, 2015, **34**, 4700-4706; f) M. Y. Lowe, S. Shu, S. M. Quan and P. L. Diaconescu, *Inorg. Chem. Frontiers*, 2017, **4**, 1798-1805; g) S. M. Quan, J. Wei and P. L. Diaconescu, *Organometallics*, 2017, **36**, 4451-4457; h) J. Wei, M. N. Riffel and P. L. Diaconescu, *Macromolecules*, 2017, **50**, 1847-1861; i) R. Dai, A. Lai, A. N. Alexandrova and P. L. Diaconescu, *Organometallics*, 2018, **37**, 4040-4047.

6. a) C. K. A. Gregson, V. C. Gibson, N. J. Long, E. L. Marshall, P. J. Oxford and A. J. P. White, *J. Am. Chem. Soc.*, 2006, **128**, 7410-7411; b) L. A. Brown, J. L. Rhinehart and B. K. Long, *ACS Catal.*, 2015, **5**, 6057-6060.

7. J. L. Brosmer and P. L. Diaconescu, *Organometallics*, 2015, **34**, 2567-2572.

8. a) N. Fey, M. F. Haddow, J. N. Harvey, C. L. McMullin and A. G. Orpen, *Dalton Trans.*, 2009, 8183-8196; b) J. Jover, N. Fey, J. N. Harvey, G. C. Lloyd-Jones, A. G. Orpen, G. J. J. Owen-Smith, P. Murray, D. R. J. Hose, R. Osborne and M. Purdie, *Organometallics*, 2010, **29**, 6245-6258; c) J. Jover, N. Fey, J. N. Harvey, G. C. Lloyd-Jones, A. G. Orpen, G. J. J. Owen-Smith, P. Murray, D. R. J. Hose, R. Osborne and M. Purdie, *Organometallics*, 2012, **31**, 5302-5306; d) N. Fey, *Chem. Cent. J.*, 2015, **9,** 38.

9. O. J. S. Pickup, I. Khazal, E. J. Smith, A. C. Whitwood, J. M. Lynam, K. Bolaky, T. C. King, B. W. Rawe and N. Fey, *Organometallics*, 2014, **33**, 1751-1761.

10. a) N. Fey, A. C. Tsipis, S. E. Harris, J. N. Harvey, A. G. Orpen and R. A. Mansson, *Chem. Eur. J.*, 2006, **12**, 291-302; b) R. A. Mansson, A. H. Welsh, N. Fey and A. G. Orpen, *J. Chem. Inf. Model.*, 2006, **46**, 2591-2600.

11. J. D. Moseley and P. M. Murray, *J. Chem. Tech. Biotech.*, 2014, **89**, 623-632.